# Effect of a free surface in ion backscattering and sputtering

H. M. Urbassek and M. Vicanek
*Institut für Theoretische Physik, Technische Universität, D-3300 Braunschweig, Federal Republic of Germany*
(Received 28 May 1987; revised manuscript received 25 November 1987)

The transport equation for the slowing down of an energetic particle in matter is solved in a $P_1$ approximation, both for a half space and for an infinite medium. Nuclear stopping with a power-law dependence on energy is assumed. The existence of the target surface affects the range distribution near the surface and the asymptotic energy spectrum of backscattered particles. In a half space, the range distribution decreases to zero at the surface and the backscattered particle spectrum is flatter than in the infinite medium. For the case of recoil generation, the analogous results for the deposited-energy distribution and the spectrum of sputtered recoils are derived. Explicit results are given for the case of hard-sphere cross sections with a power-law dependence on energy.

## I. INTRODUCTION

The phenomena associated with the slowing down of an energetic atom or ion in matter have been studied extensively in the past,[1] and many quantities like the range distribution of implanted atoms[2] and the energy spectrum of backscattered projectiles[3] are by now well understood.[4] The case when the projectile initiates a recoil cascade in the target has been studied analogously, and the damage or deposited-energy distribution[5] and the spectrum of sputtered recoils[6] have been calculated. Analytical progress in this area has depended to a large extent on simplifying the target geometry such that the slowing-down process is often considered to take place in an infinite medium. In this case the linear transport equations describing the flux of the implanted and recoiling atoms are readily solved by taking spatial moments. The reconstruction of the space dependence of the flux from its moments is not a trivial problem, but may be performed with sufficient success.[5]

In some problems, however, a more detailed knowledge of the spatial dependence of the fluxes of moving atoms in the target is desirable. Examples are the calculation of the tails of the fluxes far inside the target[7] or the description of slowing down and range profiles in layered targets.[8] Another outstanding problem is the question of how the process of particle slowing down and recoil generation in the target is affected by the existence of the target surface. This surface effect is of decisive importance for the energy and angular distribution of backscattered or sputtered particles since these are given by the fluxes through the surface itself. But also the range and energy deposition profiles in the vicinity of the surface may be modified due to the surface.

A number of investigations have studied the surface effect via a sort of perturbation approach, starting from the infinite-medium solution, or via an image type of argument. Corrections to the backscattering[9,10] and sputtering yields and spectra,[6,11] as well as to the range and deposited-energy distributions,[12,13] have been discussed in more or less detail. A few model solutions using synthetic scattering cross sections discuss the surface effect in a more detailed manner.[14]

The present investigation is motivated by an approach by Winterbon[15] who uses what is called a $P_1$ approximation to the particle flux to calculate the range distribution, reflection coefficient, and backscattering spectrum of projectiles. We extend his results and show that the range and deposited-energy distributions vanish at the target surface in a nonanalytical way, and that the energy spectra of backscattered and sputtered particles deviate characteristically from their infinite-medium values for not too small bombardment energies. Both facts are intimately connected. For a certain form of particle interaction, viz., that of energy-dependent hard spheres, we give analytical results for the range distribution and energy spectra.

## II. EQUATIONS AND $P_1$ APPROXIMATION

In this section, we introduce the formalism to describe the motion of an energetic projectile in matter; we closely follow standard notation.[15] The extension to include recoil generation is straightforward and will be presented in Sec. VII.

Consider a beam of projectile atoms or ions of mass $M_1$ slowing down in a target consisting of randomly distributed atoms of mass $M_2$. A forward transport equation is readily written down for the phase-space density $f(\mathbf{r},E,\mathbf{\Omega})$ of particles moving at point $\mathbf{r}$ with energy $E$ into direction $\mathbf{\Omega}$:[7,14]

$$v\mathbf{\Omega}\cdot\frac{\partial}{\partial\mathbf{r}}f(\mathbf{r},E,\mathbf{\Omega})=N\int dE'd^2\Omega'[K(E',\mathbf{\Omega}'\rightarrow E,\mathbf{\Omega})v'f(\mathbf{r},E',\mathbf{\Omega}')-K(E,\mathbf{\Omega}\rightarrow E',\mathbf{\Omega}')vf(\mathbf{r},E,\mathbf{\Omega})]+S(\mathbf{r},E,\mathbf{\Omega})\ . \quad (1)$$

 

Here, $N$ is the target-atom number density, $v=(2E/M_1)^{1/2}$ the projectile velocity, and $S$ denotes the stationary projectile sources. Furthermore, $K(E,\Omega \rightarrow E',\Omega')dE'd^2\Omega'$ is the scattering cross section for a projectile of energy $E$ and direction $\Omega$ to scatter at a resting target atom into energy $E'$ and direction $\Omega'$; it may be written explicitly as

$$K(E,\Omega\rightarrow E',\Omega')dE'd^2\Omega' = \sigma(E,T)dT\frac{1}{2\pi}\delta(\Omega\cdot\Omega'-\hat{\mu})d^2\Omega' , \quad (2)$$

where $T=E-E'$ is the transferred energy and $\hat{\mu}$ is the cosine of the projectile deflection angle; $\sigma(E,T)dT$ is the cross section for energy transfer $T$ in its usual notation.[1]

In the following, we shall be interested in a planar geometry; we denote by $z$ the depth into the target, and by $\mu$ the direction cosine of $\Omega$ with respect to the inward target normal, i.e., the $z$ axis. For a stationary and homogeneous beam of current density $\psi$ (particles per unit time and area), the source may be written as

$$S(\mathbf{r},E,\Omega)=\psi Q(z,E,\mu) , \quad (3)$$

where cylindrical symmetry was assumed. We now introduce the projectile flux by

$$\Phi(z,E,\mu)=\frac{1}{\psi}vf(\mathbf{r},E,\Omega) . \quad (4)$$

Expanding $\Phi$ into Legendre polynomials

$$\Phi(z,E,\mu)=\sum_{l=0}^{\infty}(2l+1)P_l(\mu)\Phi_l(z,E) ,$$
$$\Phi_l(z,E)=\tfrac{1}{2}\int_{-1}^{1}d\mu\, P_l(\mu)\Phi(z,E,\mu) , \quad (5)$$

Eq. (1) becomes (for details see Ref. 5)

$$\frac{\partial}{\partial z}[\mu\Phi(z,E,\mu]_l = N\int dE'[\sigma(E',E'-E)P_l(\hat{\mu})\Phi_l(z,E') - \sigma(E,E-E')\Phi_l(z,E)] + Q_l(z,E) , \quad (6)$$

where $[F(\mu)]_l$ denotes the $l$th Legendre moment of an arbitrary function $F(\mu)$, in accordance with Eq. (5).

We attempt to solve Eq. (6) in a $P_1$ approximation which consists in restricting the $\mu$ variation of $\Phi(z,E,\mu)$ to

$$\Phi(z,E,\mu)=\Phi_0(z,E)+3\mu\Phi_1(z,E) \quad (7)$$

and neglecting higher-order Legendre moments, i.e., the infinite expansion (5) is truncated after the $P_1$ term, whence the name. Equation (6) is then reduced to a coupled system of two integro-differential equations.

We shall solve the above equations for scattering cross sections that obey a power law:

$$\sigma(E,T)dT=CE^{-2m}g\left(\frac{T}{E}\right)\frac{dT}{E} , \quad (8)$$

for $0<T<\gamma E$ (otherwise, $\sigma$ vanishes), and $\gamma=4M_1M_2/(M_1+M_2)^2$. Here $0\le m\le 1$, and $g(T/E)$ measures the degree of forward scattering in a single collision. The choice $g(t)=t^{-1-m}$ is a convenient approximation for scattering in a potential $V(r)\propto r^{-1/m}$.[1,6] Another model cross section which has been considered in the literature is $g(t)\equiv 1$, which denotes hard-sphere scattering with an energy-dependent scattering cross section.[16,17]

When inserting (8) into (6), it is convenient to scale the depth variable $z$ to a length characteristic of the bombarding particle:

$$x=\frac{z}{\lambda_0},\quad \lambda_0=\frac{E_0^{2m}}{\gamma NC} , \quad (9)$$

and to scale the particle energy $E$ to the bombarding energy $E_0$:

$$\varepsilon=E/E_0 . \quad (10)$$

Thus from now on the nondimensional flux and sources

$$\Phi(x,\varepsilon,\mu)=E_0\Phi(z=x\lambda_0,E=\varepsilon E_0,\mu) ,$$
$$Q(x,\varepsilon,\mu)=\lambda_0E_0Q(z=x\lambda_0,E=\varepsilon E_0,\mu) , \quad (11)$$

will be used. Finally, after a (finite) Mellin transformation in $\varepsilon$:

$$\Phi(x,s,\mu)=\int_0^1 d\varepsilon\,\varepsilon^{s-1}\Phi(x,\varepsilon,\mu) , \quad (12)$$

Eq. (6) reads, in the $P_1$ approximation,

$$\frac{\partial}{\partial x}\Phi_1(x,s)=-A_0(s)\Phi_0(x,s-2m)+Q_0(x,s) ,$$
$$\frac{1}{3}\frac{\partial}{\partial x}\Phi_0(x,s)=-A_1(s)\Phi_1(x,s-2m)+Q_1(x,s) , \quad (13)$$

with

$$A_l(s)=\frac{1}{\gamma}\int_0^{\gamma}dt\,g(t)[1-(1-t)^{s-1}P_l(\hat{\mu})] \quad (14)$$

and

$$\hat{\mu}(t)=(1-t)^{-1/2}\left[1-\frac{M_1+M_2}{2M_1}t\right] . \quad (15)$$

In an infinite medium, the stationary unit source injects particles into the target as $Q(z,E,\mu)=\delta(z)\delta(E-E_0)\delta(\mu-\mu_0)$. In the $P_1$ formalism, this reduces to

$$Q_l(x,s)=\tfrac{1}{2}\delta(x)P_l(\mu_0) , \quad (16a)$$

($l=0,1$) and is supplemented by the boundary conditions

$$\Phi_l(x\rightarrow\pm\infty,s)\equiv 0 . \quad (16b)$$

A half space may be described by either of the following approaches: One may retain the same source $Q(z,E,\mu)$ as in the infinite medium and additionally stipulate that no particles from the outside enter the half space: $Q(z=0,E,\mu>0)\equiv 0$; alternatively, one may put the incident current into the boundary conditions, demanding

$$\Phi(z=0,E,\mu>0)=\frac{1}{\mu_0}\delta(E-E_0)\delta(\mu-\mu_0) , \quad (17)$$

and setting the source $Q(z,E,\mu)\equiv 0$. Both approaches

give identical results when applied to the original transport equation (1) or (6),[18] but certainly not when applied to the $P_1$ approximation (13). For the purposes of the present paper, we choose the latter alternative, since it gives more succinct results. We note explicitly, though, that the main qualitative results of the present paper may be obtained by either approach.

In the $P_1$ approximation, (17) can certainly not be fulfilled rigorously; the boundary condition is usually implemented using Marshak's condition:[18]

$$\int_0^1 d\mu\,\mu\Phi(z=0,E,\mu)=\tfrac{1}{2}\Phi_0(z=0,E)+\Phi_1(z=0,E) =\delta(E-E_0)\ . \tag{18}$$

Thus, for the half-space problem, Eq. (13) is supplemented by

$$\begin{aligned} &Q_l(x,s)\equiv 0\ , \\ &\tfrac{1}{2}\Phi_0(x=0,s)+\Phi_1(x=0,s)\equiv 1\ , \\ &\Phi_l(x\to+\infty,s)\equiv 0\ . \end{aligned} \tag{19}$$

We note that no information on the incident direction $\mu_0$ is retained in this half-space formulation of the $P_1$ approximation.

## III. SOLUTION

We solve the coupled system of difference differential equations (13) using Waller's trick.[19,14,15] Write

$$\Phi_l(x,s)=D_l(s)X_l(x,s)\ , \tag{20}$$

where the $D_l(s)$ satisfy

$$\begin{aligned} D_0(s)&=-A_1(s)D_1(s-2m)\ , \\ D_1(s)&=-A_0(s)D_0(s-2m)\ . \end{aligned} \tag{21}$$

Then

$$\begin{aligned} &\frac{\partial}{\partial x}X_1(x,s)=X_0(x,s-2m)+\frac{1}{D_1(s)}Q_0(x,s)\ , \\ &\frac{1}{3}\frac{\partial}{\partial x}X_0(x,s)=X_1(x,s-2m)+\frac{1}{D_0(s)}Q_1(x,s)\ , \end{aligned} \tag{22}$$

which is readily solved using the Laplace transform:

$$X_l(x,s)=\int_0^\infty dv\,e^{-sv}Y_l(x,v)\ . \tag{23}$$

For a monoenergetic source, $Q$ is independent of $s$ and we obtain

$$\begin{aligned} &\frac{\partial}{\partial x}Y_1(x,v)=e^{2mv}Y_0(x,v)+T_1(v)Q_0(x)\ , \\ &\frac{1}{3}\frac{\partial}{\partial x}Y_0(x,v)=e^{2mv}Y_1(x,v)+T_0(v)Q_1(x)\ , \end{aligned} \tag{24}$$

and

$$\frac{1}{D_l(s)}=\int_0^\infty dv\,e^{-sv}T_l(v)\ . \tag{25}$$

For the infinite-medium problem we get

$$\begin{aligned} Y_0(x,v)&=\tfrac{3}{4}e^{-k|x|}\left[-\frac{T_1(v)}{\sqrt{3}}+\mu_0 T_0(v)\mathrm{sgn}x\right]\ , \\ Y_1(x,v)&=\tfrac{3}{4}e^{-k|x|}\left[-\mu_0\frac{T_0(v)}{\sqrt{3}}+\tfrac{1}{3}T_1(v)\mathrm{sgn}x\right]\ , \end{aligned} \tag{26}$$

and for the half space

$$\begin{aligned} Y_0(x,v)&=b(v)e^{-kx}\ , \\ Y_1(x,v)&=-\frac{1}{\sqrt{3}}Y_0(x,v)\ . \end{aligned} \tag{27}$$

Here

$$k=k(v)=\sqrt{3}e^{2mv}\ , \tag{28}$$

and $b(v)$ is the Laplace inverse of

$$b(s)=\int_0^\infty dv\,e^{-sv}b(v)=\frac{1}{\frac{1}{2}D_0(s)-\frac{1}{\sqrt{3}}D_1(s)}\ . \tag{29}$$

From (20) and (23), the solution of the system (13) is now obtained as

$$\Phi_l(x,s)=D_l(s)\int_0^\infty dv\,e^{-sv}Y_l(x,v)\ . \tag{30}$$

## IV. ENERGY SPECTRUM

The Mellin-transformed energy spectrum of emitted particles is given in the infinite medium by

$$\begin{aligned} \Phi_0(x=0,s)&=-\frac{\sqrt{3}}{4}\frac{D_0(s)}{D_1(s)}\ , \\ \Phi_1(x=0,s)&=-\frac{\sqrt{3}}{4}\mu_0\frac{D_1(s)}{D_0(s)}\ , \end{aligned} \tag{31}$$

and in the half space by

$$\begin{aligned} \Phi_0(x=0,s)&=\frac{D_0(s)}{\frac{1}{2}D_0(s)-\frac{1}{\sqrt{3}}D_1(s)}\ , \\ \Phi_1(x=0,s)&=-\frac{1}{\sqrt{3}}\frac{D_1(s)}{\frac{1}{2}D_0(s)-\frac{1}{\sqrt{3}}D_1(s)}\ . \end{aligned} \tag{32}$$

In order to assess the rightmost poles of $\Phi_l(x=0,s)$, which give us the asymptotic energy dependence of $\Phi_l(x=0,E)$ for $E\ll E_0$, we have to study in some detail the analytical properties of the $D_l(s)$. From (21) we have

$$\begin{aligned} D_0(s+4m)&=A_1(s+4m)A_0(s+2m)D_0(s)\ , \\ D_1(s+4m)&=A_0(s+4m)A_1(s+2m)D_1(s)\ . \end{aligned} \tag{33}$$

Consider first the case of different projectile and target masses, $\gamma<1$. Then, by definition, all $A_l(s)$ are entire functions, and they have no poles in the $s$ plane. Therefore the rightmost poles of the $D_l(s)$ are caused by the rightmost zeroes of the $A_l(s)$, with different $l$. $A_0(s)$ has its rightmost zero at $s=1$, whereas $A_1(s)$ has its rightmost zero at another point $\sigma$ on the real axis, with $\sigma<1$. From (33), it follows that the rightmost pole of $D_0(s)$ is at

$s=1-2m$, and that of $D_1(s)$ is at $s_1=\max(1-4m, \sigma-2m)$. Hence, we obtain the asymptotic behavior of the infinite-medium solution, Eq. (31):

$$\Phi_0(x=0,\varepsilon)\sim\varepsilon^{-(1-2m)}, \quad \varepsilon\ll 1$$
$$\Phi_1(x=0,\varepsilon)\sim\varepsilon^{-s_1}, \quad \varepsilon\ll 1 . \tag{34}$$

Note that for small $m$, $s_1=1-4m$.

In the case of equal projectile and target mass, $\gamma=1$, the $A_l(s)$ are no longer entire functions, and we have to show that the poles of the $A_l(s)$ do not change the asymptotics (34). $A_0(s)$ has its rightmost pole at $s=0$, and $A_1(s)$ at $s=-\frac{1}{2}$. Therefore $D_0(s)$ has its rightmost zero at $s=-2m$, and $D_1(s)$ at $s=\max(-4m,-\frac{1}{2}-2m)$. Thus these zeroes are not relevant for the asymptotics of the energy spectra, and again Eq. (34) holds.

We note that the two spatial moments

$$\Phi_0^0(s)=\int_{-\infty}^{+\infty}dx\,\Phi_0(x,s)=\frac{1}{2A_0(s+2m)} ,$$
$$\Phi_1^0(s)=\int_{-\infty}^{+\infty}dx\,\Phi_1(x,s)=\frac{\mu_0}{2A_1(s+2m)} \tag{35}$$

are calculated correctly in the $P_1$ approximation.[18] We observe that in the infinite medium, the spatial mean of the density $\Phi_0^0(E)$ has the same asymptotic energy dependence as $\Phi_0(x=0,E)$ evaluated at the surface. For the current $\Phi_1$ this is not necessarily true; for small $m$ in particular, $\Phi_1^0(E)$ will underestimate $\Phi_1(x=0,E)$. The reason hereto is that $\Phi_1(x,E)$ generally changes sign as a function of $x$ and is negative at the surface while its mean is positive.[20]

The above discussion is summarized in Fig. 1 where the behavior of $D_1(s)/D_0(s)$, which determines the asymptotics of the infinite-medium solution, is sketched. We used the fact that because of Eq. (21) and since $\lim_{s\to\infty}[A_0(s)/A_1(s)]=1$, it follows $\lim_{s\to\infty}[D_1(s)/D_0(s)]=-1$.

For the half-space solution, the pole of $D_0(s)$ at $s=1-2m$ is irrelevant. As neither $D_0(s)$ nor $D_1(s)$ have a pole to the right of $s_1$, obviously one has to look for the zeroes of the denominator of Eq. (32), $\frac{1}{2}D_0(s)-(1/\sqrt{3})D_1(s)$. As sketched in Fig. 1 there is indeed one and only one zero of the denominator of the half-space solution for $\mathrm{Re}\,s>s_1$, which we will call $s_0$:

$$\frac{D_1(s_0)}{D_0(s_0)}=\frac{\sqrt{3}}{2} . \tag{36}$$

Thus in the half space $\Phi_0$ and $\Phi_1$ possess the same asymptotics; it is

$$\Phi_{0,1}(x=0,\varepsilon)\sim\varepsilon^{-s_0}, \quad \varepsilon\ll 1 . \tag{37}$$

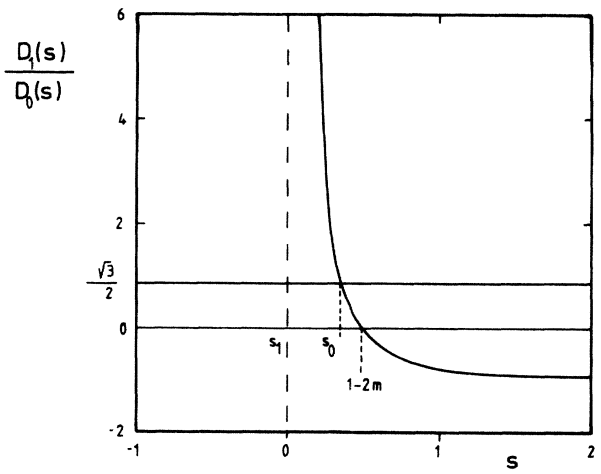


FIG. 1. A sketch of the behavior of $D_1(s)/D_0(s)$ for real $s$, $s>s_1$. Values are taken for the case of hard-sphere scattering with $m=\frac{1}{4}$, Eq. (66). See text.

Note that this asymptotics is in between that of the infinite-medium density $\Phi_0(x=0,\varepsilon)$ and current $\Phi_1(x=0,\varepsilon)$:

$$s_1<s_0<1-2m . \tag{38}$$

Furthermore, since $\Phi_1(x=0,\varepsilon)/\Phi_0(x=0,\varepsilon)$ does not vanish for $\varepsilon\to 0$, the angular distribution of emitted particles does not become isotropic at low emission energies, in contrast to the infinite-medium solution, Eq. (34).

## V. REFLECTION AND STICKING COEFFICIENTS

In order to discuss reflection and sticking coefficients, and to calculate the range distribution from the particle flux, it is convenient to introduce the slowing-down density[21,14] $\chi(\mathbf{r},E)$. It corresponds to the so-called Brice distribution function utilized in other work on half-space ranges and spectra.[10,12] $\chi$ is defined as

$$\chi(\mathbf{r},E)=-\int_E^{E_0}dE'\int d^2\Omega'\left[\frac{\partial f(\mathbf{r},E',\Omega')}{\partial t}\right]_{\mathrm{coll}} . \tag{39}$$

Here $(\partial f(\mathbf{r},E,\Omega)/\partial t)_{\mathrm{coll}}$ is used as an abbreviation of the right-hand side of Eq. (1) (without sources); it means the time rate of change of $f(\mathbf{r},E,\Omega)$ due to collisions. Since we deal exclusively with down scattering, $\chi(\mathbf{r},E)d^3r$ denotes the number of particles scattered down through energy $E$ at point $(\mathbf{r},d^3r)$ per unit time irrespective of direction. In planar geometry, we have

$$\chi(z,E)=-2\int_E^{E_0}dE'N\int_0^{E_0}dE''[\sigma(E'',E''-E')\Phi_0(z,E'')-\sigma(E',E'-E'')\Phi_0(z,E')] . \tag{39'}$$

For the cross section (8) we change to the nondimensional depth variable, Eq. (9):

$$\chi(x,\varepsilon)=\lambda_0\chi(z=x\lambda_0,E=\varepsilon E_0) \tag{40}$$

and obtain after Mellin transformation in $\varepsilon$, cf. Eq. (12),

$$\chi(x,s)=2\frac{A_0(s+1)}{s}\Phi_0(x,s+1-2m) . \tag{41}$$

Particles scattering down through energy $E=0$ define the range distribution. It is well defined if $s=0$ is the highest pole of $\chi(x,s)$; then[15]

$$R(x)=\operatorname*{Res}_{s=0}\chi(x,s)=2\lim_{s\to 1}[A_0(s)\Phi_0(x,s-2m)] . \tag{42}$$

From Eq. (6) we observe that the important continuity equation holds

$$\frac{\partial j(x,\varepsilon)}{\partial x}-\frac{\partial}{\partial\varepsilon}\chi(x,\varepsilon)=Q(x,\varepsilon) , \tag{43}$$

where

$$j(x,\varepsilon)=2\Phi_1(x,\varepsilon) \tag{44}$$

is the nondimensional particle current, and $Q(x,\varepsilon)=\int d\mu\, S(x,\varepsilon,\mu)$ the angle-integrated source. It allows us to define the reflection coefficient $r$ and the sticking coefficient $a$ by

$$\begin{aligned} r&=-\int_0^{1^-}d\varepsilon\, j(x=0,\varepsilon)\\ &=-2[\Phi_1(x=0,s=1)-\Phi_1(x=0,s\to\infty)] , \end{aligned} \tag{45}$$

$$a=\int_0^{\infty}dx\, R(x)=-2D_1(s=1)\int_0^{\infty}dx\, X_0(x,s=1-2m) ,$$

which satisfy in view of Eq. (43) the obvious relationship

$$r+a=j_{\rm in}=\int_{1^-}^{1}d\varepsilon\, j(x=0,\varepsilon)=2\Phi_1(x=0,s\to\infty) . \tag{46}$$

The symbol $1^-$ in the integration limit is introduced here in order to separate the contributions of the source at $\varepsilon=1$ from the backscattered particles at $\varepsilon<1$. If sources $Q(x)\propto\delta(x)$ are present, $x=0^+$ is to be taken in Eqs. (45) and (46). For the infinite-medium solution (26) we get

$$\begin{aligned} j_{\rm in}&=\tfrac{1}{2}(1+\sqrt{3}\mu_0) ,\\ a&=\frac{1}{2}\left[1-\sqrt{3}\mu_0\frac{D_1(1)}{D_0(1)}\right] ,\\ r&=\frac{\sqrt{3}}{2}\mu_0\left[1+\frac{D_1(1)}{D_0(1)}\right] . \end{aligned} \tag{47}$$

Furthermore, it holds independently of $\mu_0$ that

$$\int_{-\infty}^{\infty}dx\, R(x)=1 . \tag{48}$$

We wish to retain the normalization (48), but also stipulate the condition (46), $r+a=1=j_{\rm in}$; both requirements may be accommodated for the bombardment direction $\mu_0=1/\sqrt{3}$, i.e., for this bombardment direction the $P_1$ approximation is best.[15,18] In future we specialize our results for sticking and reflection coefficients to $\mu_0=1/\sqrt{3}$.

In the half space, it is

$$\begin{aligned} j_{\rm in}&=8\left[1-\frac{\sqrt{3}}{2}\right] ,\\ a&=\frac{2}{1-\frac{\sqrt{3}}{2}\frac{D_0(1)}{D_1(1)}} ,\\ r&=j_{\rm in}-a . \end{aligned} \tag{49}$$

Here we wish again to normalize $a+r=1=j_{\rm in}$, and we thus use in future the flux

$$\Phi_l^{\rm HS}(x,\varepsilon)=\frac{1}{j_{\rm in}}\Phi_l(x,\varepsilon) \tag{50}$$

as the true half-space result.

## VI. RANGES

The range distribution is obtained via Eq. (42) from the particle flux $\Phi$. Whereas the infinite-medium range in general does not vanish at $x=0$, it is our purpose to show in this section that the half-space range decreases to zero at $x=0$. For an analysis of the latter it is convenient to introduce the spatial Mellin transform

$$\Phi_l^{\rm HS}(p,s)=\int_0^{\infty}dx\, x^{p-1}\Phi_l^{\rm HS}(x,s) . \tag{51}$$

It is

$$\begin{aligned} \Phi_0^{\rm HS}(p,s)&=\frac{D_0(s)}{j_{\rm in}}\frac{\Gamma(p)3^{-p/2}}{\frac{1}{2}D_0(s+2mp)-\frac{1}{\sqrt{3}}D_1(s+2mp)} ,\\ \Phi_1^{\rm HS}(p,s)&=-\frac{1}{\sqrt{3}}\frac{D_1(s)}{D_0(s)}\Phi_0^{\rm HS}(p,s) , \end{aligned} \tag{52}$$

and thus the Mellin-transformed range distribution is

$$R(p)=-2\frac{D_1(1)}{j_{\rm in}}\frac{\Gamma(p)3^{-p/2}}{\frac{1}{2}D_0(1+2m(p-1))-\frac{1}{\sqrt{3}}D_1(1+2m(p-1))} . \tag{53}$$

As was shown above, $D_0(s)$ has its rightmost pole at $s=1-2m$, and the rightmost zero of the denominator $\frac{1}{2}D_0(q)-(1/\sqrt{3})D_1(q)$ is at $q=s_0$, where $1-4m\le s_1<s_0<1-2m$. Hence $R(p)$ is regular at $p=0$, and possesses poles at $p=-\rho_i$ only in the negative half plane ($\rho_i>0$). We thus get an expansion

$$\begin{aligned} R(x)&=-2\frac{D_1(1)}{j_{\rm in}}\sum_{i=0}^{\infty}C_i x^{\rho_i} ,\\ C_i&=\operatorname*{Res}_{p=-\rho_i}\frac{\Gamma(p)3^{-p/2}}{\frac{1}{2}D_0(1+2m(p-1))-\frac{1}{\sqrt{3}}D_1(1+2m(p-1))} , \end{aligned} \tag{54}$$

where the leading term for small $x$ is

$$R(x)\propto x^{\rho}\ , \qquad \rho=\rho_0=\frac{1-2m-s_0}{2m},\quad 0<\rho<1\ , \tag{55}$$

and $s_0$ is given by Eq. (36).

We conclude that the half-space range distribution vanishes at the surface like a power $x^{\rho}$ with $0<\rho<1$.

## VII. RECOIL FLUX

While the projectile slows down in collisions with target atoms, it shares its energy with the recoiling atoms which in their turn collide with other target atoms, etc. In this way a recoil cascade may build up. A transport equation describing the recoil atom phase-space density $f^{\rm rec}(\mathbf{r},E,\mathbf{\Omega})$ and the recoil flux $\Psi(z,E,\mu)$ is set up in complete analogy to that for the projectile phase-space density $f$ and flux $\Phi$, the only difference being that to the collision term on the right-hand side of Eq. (1), a recoil term

$$+N\int dE'd^2\Omega' K^{\rm rec}(E',\mathbf{\Omega}'\rightarrow E\mathbf{\Omega})v' f^{\rm rec}(\mathbf{r},E',\mathbf{\Omega}') \tag{1'}$$

is added. $K^{\rm rec}(E',\mathbf{\Omega}'\rightarrow E,\mathbf{\Omega})$ denotes the cross section for a particle of energy $E'$ and direction $\mathbf{\Omega}'$ to scatter at a resting target atom and impart to it energy $E$ and direction $\mathbf{\Omega}$. In general the source term for recoil particles depends on the projectile flux. For the case of self-sputtering we need not distinguish between projectile and target species, and the flux of all moving atoms may be described by $\Psi$. We will concentrate on this case.

The $P_1$ equations for the recoil flux are then again given by Eqs. (13), with the boundary conditions given by (16a) and (16b) for the infinite medium, and by (19) for the half space. The only difference is that the collision terms $A_l(s)$, due to the inclusion of the recoil term, are substituted by

$$A_l^{\rm rec}(s)=\int_0^1 dt\, g(t)[\,1-P_l(\sqrt{1-t}\,)(1-t)^{s-1} -P_l(\sqrt{t}\,)t^{s-1}]\ . \tag{14'}$$

Since $A_0^{\rm rec}(s=2)=0$, we obtain for an infinite medium

$$\Psi_0(x=0,\varepsilon)\sim\varepsilon^{-(2-2m)},\quad \varepsilon\ll 1$$
$$\Psi_1(x=0,\varepsilon)\sim\varepsilon^{-s_1},\quad \varepsilon\ll 1\ , \tag{56}$$

where $s_1=\max(2-4m,\sigma-2m)$ and $\sigma$ is the rightmost zero of $A_1^{\rm rec}(s)$. For the half space,

$$\Psi_{0,1}(x=0,\varepsilon)\sim\varepsilon^{-s_0},\quad \varepsilon\ll 1\ , \tag{57}$$

where $s_1<s_0<2-2m$, and

$$\frac{D_1(s_0)}{D_0(s_0)}=\frac{\sqrt{3}}{2}\ .$$

We use here the same symbols as in the projectile case in order to emphasize the complete analogy of the two problems.

In analogy to the current $j$ and the slowing-down density $\chi$, we now introduce the energy current density

$$j_E(z,\varepsilon)=2\varepsilon\Psi_1(z,\varepsilon)\ , \tag{58}$$

and the slowing-down energy density[14] $\omega(\mathbf{r},E)$, defined as the amount of energy slowing down through energy $E$ at $(\mathbf{r},d^3r)$:

$$\omega(\mathbf{r},E)=-\int_E^{E_0} dE'd^2\Omega' E'\left[\frac{\partial f^{\rm rec}(\mathbf{r},E',\mathbf{\Omega}')}{\partial t}\right]_{\rm coll}\ , \tag{59}$$

where now $(\partial f^{\rm rec}/\partial t)_{\rm coll}$ denotes the right-hand side of Eq. (1) augmented by the recoil term (1'). For planar geometry, and in nondimensional units, we have

$$\omega(x,\varepsilon)=\frac{\lambda_0}{\psi E_0}\omega(\mathbf{r},E)\ . \tag{59'}$$

In case of negligible electronic stopping, $\omega$ obeys the continuity equation

$$\frac{\partial}{\partial x}j_E(x,\varepsilon)-\frac{\partial}{\partial\varepsilon}\omega(x,\varepsilon)=\varepsilon Q(x,\varepsilon)\ . \tag{60}$$

In Mellin space, it is

$$\omega(x,s)=2\frac{A_0^{\rm rec}(s+2)}{s}\Psi_0(x,s+2-2m)\ . \tag{61}$$

The distribution of deposited energy is then given by

$$F(x)=\omega(x,\varepsilon=0)=\lim_{s\rightarrow 2}[\,A_0^{\rm rec}(s)\Psi_0(x,s-2m)]\ . \tag{62}$$

In the half space, we obtain the expansion for small $x$:

$$F(x)\propto x^{\rho}\ , \qquad \rho=\frac{2-2m-s_0}{2m},\quad 0<\rho<1\ . \tag{63}$$

## VIII. AN EXAMPLE

We have not been able to solve the difference equations (21) for a general cross section (8) other than in a formal way. Certainly, a numerical solution is always possible; for the purposes of the present paper, however, it appears more appropriate to study a case where an analytical solution is available. For the equal mass case $M_1=M_2$ and hard-sphere scattering $g(t)\equiv 1$, the collision terms $A_l(s)$ become rational functions, which fact allows an easy analytical solution of Eqs. (21). As an illustration we will present the solutions for the projectile distributions for this case. We have

$$A_0(s)=\frac{s-1}{s},\quad A_1(s)=\frac{s-\frac{1}{2}}{s+\frac{1}{2}}\ , \tag{64}$$

and the difference equations (21) have the solution

$$D_0(s)=\frac{\Gamma\left[\frac{s+2m-1}{4m}\right]\Gamma\left[\frac{s+4m-\frac{1}{2}}{4m}\right]}{\Gamma\left[\frac{s+2m}{4m}\right]\Gamma\left[\frac{s+4m+\frac{1}{2}}{4m}\right]}\ ,$$
$$D_1(s)=-\frac{\Gamma\left[\frac{s+4m-1}{4m}\right]\Gamma\left[\frac{s+2m-\frac{1}{2}}{4m}\right]}{\Gamma\left[\frac{s+4m}{4m}\right]\Gamma\left[\frac{s+2m+\frac{1}{2}}{4m}\right]}\ . \tag{65}$$

These functions become particularly simple for $m=1/4n$, $n=1,2,3,\ldots$. Let us specialize to $m=\frac{1}{4}$. Then

$$D_0(s)=\frac{1}{(s-\frac{1}{2})(s+\frac{1}{2})},\quad D_1(s)=-\frac{1}{s^2}\ . \tag{66}$$

For better readability, we will in this section use the abbreviation

$$\xi=\sqrt{3}x \tag{67}$$

for the depth variable. The infinite-medium solution then reads

$$\begin{aligned}\Phi_0(x,s)&=\frac{\sqrt{3}}{4}e^{-|\xi|}D_0(s)\\&\quad\times\{\alpha(\xi,s)+[\alpha(\xi,s)-\tfrac{1}{4}]\sqrt{3}\mu_0\mathrm{sgn}\xi\}\ ,\\\Phi_1(x,s)&=-\tfrac{1}{4}e^{-|\xi|}D_1(s)\\&\quad\times\{\sqrt{3}\mu_0[\alpha(\xi,s)-\tfrac{1}{4}]+\alpha(\xi,s)\mathrm{sgn}\xi\}\ ,\end{aligned} \tag{68}$$

where

$$\alpha(\xi,s)=\left[s+\frac{|\xi|}{2}\right]^2-\frac{|\xi|}{4}\ . \tag{69}$$

Equations (68) may readily be Mellin-inverted analytically, but we will not use the general expression for $\Phi_l(x,\varepsilon)$ in the following. The energy spectrum at the surface reads

$$\begin{aligned}\Phi_0(x=0^+,\varepsilon)&=\frac{\sqrt{3}}{4}\left\{(1+\sqrt{3}\mu_0)\delta(\varepsilon-1)\right.\\&\qquad\left.+\frac{1}{4}(\varepsilon^{-1/2}-\varepsilon^{1/2})\right\},\\\Phi_1(x=0^+,\varepsilon)&=\frac{1}{4}\left[(1+\sqrt{3}\mu_0)\delta(\varepsilon-1)-\frac{\sqrt{3}\mu_0}{4}\ln\frac{1}{\varepsilon}\right].\end{aligned} \tag{70}$$

We furthermore obtain the range distribution

$$R(x)=\frac{\sqrt{3}}{8}e^{-|\xi|}\begin{cases}(1+\sqrt{3}\mu_0)(\xi^2+\xi)+1, & x>0\\(1-\sqrt{3}\mu_0)(\xi^2-\xi)+1, & x<0\ ,\end{cases} \tag{71}$$

which is continuous and twice continuously differentiable at $x=0$. For small $\varepsilon\ll 1$ the current $\Phi_1(x,\varepsilon)$ reads

$$\Phi_1(x,\varepsilon)=\ln(1/\varepsilon)\phi_1(x)\ , \tag{72a}$$

with

$$\phi_1(x)=\tfrac{1}{16}e^{-|\xi|}\begin{cases}(\sqrt{3}\mu_0+1)(\xi^2-\xi)-\sqrt{3}\mu_0, & x>0\\(\sqrt{3}\mu_0-1)(\xi^2+\xi)-\sqrt{3}\mu_0, & x<0\ ,\end{cases} \tag{72b}$$

which is the leading term of an asymptotic expansion for $\varepsilon\ll 1$. Finally we obtain, for $\mu_0=1/\sqrt{3}$, the sticking coefficient $a$ and the reflection coefficient $r$:

$$a=\tfrac{7}{8},\quad r=\tfrac{1}{8}\ . \tag{73}$$

The half-space energy spectrum reads

$$\begin{aligned}\Phi_0^{\mathrm{HS}}(x=0,\varepsilon)&=\frac{\sqrt{3}}{2}\delta(\varepsilon-1)+\frac{\sqrt{3}}{4}s_0(\varepsilon^{-s_0}-\varepsilon^{s_0})\ ,\\\Phi_1^{\mathrm{HS}}(x=0,\varepsilon)&=\tfrac{1}{2}\delta(\varepsilon-1)-\frac{\sqrt{3}}{8}s_0(\varepsilon^{-s_0}-\varepsilon^{s_0})\ ,\end{aligned} \tag{74}$$

where the normalization (50) was employed and $s_0$ is the only positive root of $D_1(s_0)/D_0(s_0)=\sqrt{3}/2$:

$$s_0=\tfrac{1}{2}(\sqrt{3}-1)\ . \tag{75}$$

The half-space range distribution may be rigorously Mellin-inverted from Eq. (53). We obtain

$$\begin{aligned}R^{\mathrm{HS}}(x)&=\frac{\sqrt{3}}{8}[\xi^{\rho}\Gamma(3-\rho,\xi)+\xi^{2-\rho}\Gamma(1+\rho,\xi)]\\&=\frac{\sqrt{3}}{8}\left[\xi^{\rho}\Gamma(3-\rho)+\xi^{2-\rho}\Gamma(1+\rho)\right.\\&\qquad-\xi^3\sum_{n=0}^{\infty}\frac{(-\xi)^n}{n!}\left(\frac{1}{n+3-\rho}\right.\\&\qquad\left.\left.+\frac{1}{n+1+\rho}\right)\right],\end{aligned} \tag{76}$$

where

$$\Gamma(a,x)=\int_x^{\infty}dt\,t^{a-1}e^{-t}$$

denotes the incomplete gamma function,[22] and

$$\rho=1-2s_0=2-\sqrt{3}\ . \tag{77}$$

The current $\Phi_1^{\mathrm{HS}}(x,\varepsilon)$ is given (for $\varepsilon\ll 1$) by

$$\Phi_1^{\mathrm{HS}}(x,\varepsilon)=\ln(1/\varepsilon)\phi_1^{\mathrm{HS}}(x)\ , \tag{78a}$$

with

$$\begin{aligned}\phi_1^{\mathrm{HS}}(x)&=\tfrac{1}{8}[\xi^2e^{-\xi}-(\tfrac{1}{2}-s_0)\xi^{-2s_0}\Gamma(2+2s_0,\xi)\\&\qquad-(\tfrac{1}{2}+s_0)\xi^{2s_0}\Gamma(2-2s_0,\xi)]\ ;\end{aligned} \tag{78b}$$

it diverges for $x\to 0$ as

$$\Phi_1^{\mathrm{HS}}(x\to 0,\varepsilon)=-\tfrac{1}{8}\ln(1/\varepsilon)(\tfrac{1}{2}-s_0)\Gamma(2+2s_0)\xi^{-2s_0}\ . \tag{79}$$

This limit does not exist; this is connected to the fact that the energy dependence at the very target surface is stronger than logarithmic, cf. Eq. (74). Sticking and reflection coefficients for the half-space problem read

$$a^{\mathrm{HS}}=\frac{\sqrt{3}}{2},\quad r^{\mathrm{HS}}=1-\frac{\sqrt{3}}{2}\ ; \tag{80}$$

$r^{\mathrm{HS}}$ is slightly larger (about 10%) than the infinite-medium reflection coefficient $r$, Eq. (73).

We plot the energy distributions $\Phi_l(x=0,\varepsilon)$ for the infinite-medium and half-space cases in Fig. 2(a). It is seen that for $E\gtrsim\frac{1}{10}E_0$, the boundary conditions do not influence density or current. Below that energy the half-space solutions lie between the values of the infinite-medium current $\Phi_1$ and density $\Phi_0$.

In Figs. 2(b) and 2(c) we display the plots of the range and the asymptotic current distributions for both types of

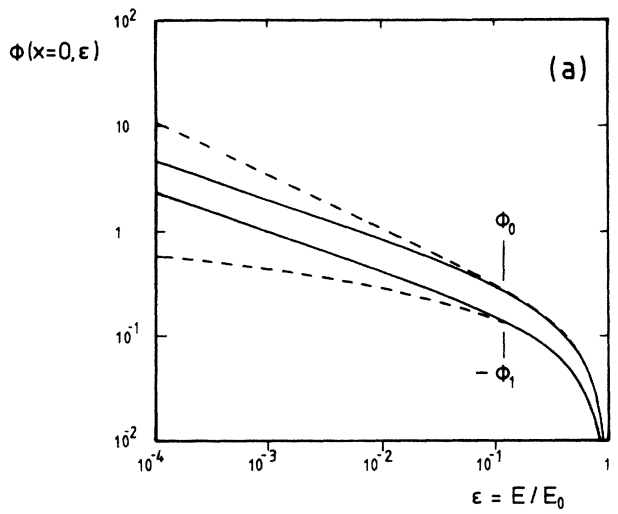


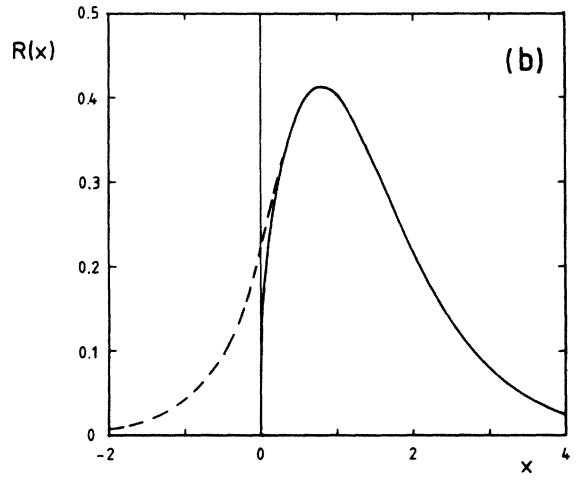


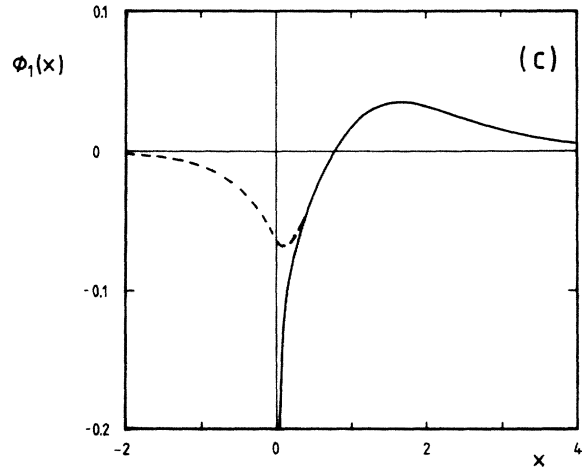


FIG. 2. Comparison of particle slowing down in a half space (solid lines) and in an infinite medium (dashed lines). The results are given for equal mass hard-sphere scattering with $m=\frac{1}{4}$. (a) Energy distributions at the surface $x=0$, Eqs. (70) and (74). (b) Range distributions, Eqs. (71) and (76). (c) Asymptotic current distributions, Eqs. (72b) and (78b).

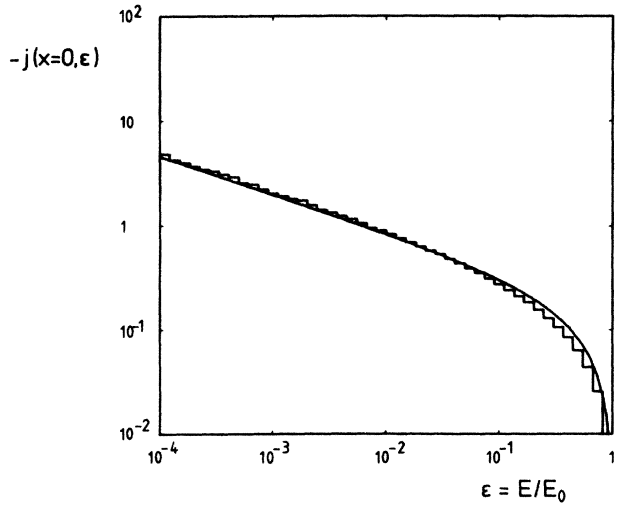


FIG. 3. Energy spectrum of particles emitted from a half space, $-j(x=0,\varepsilon)=-2\Phi_1(x=0,\varepsilon)$, for hard-sphere scattering with $m=\frac{1}{4}$. Solid lines: $P_1$ result, Eq. (74). Histogram: Monte Carlo simulation.

boundary conditions. For depths $x \gtrsim 0.5$, the boundary conditions do not influence the distributions. The range distribution goes to zero for $x \to 0$ in the half space, though, while the current distribution diverges here.

Note that for large depths, the range distributions for the infinite medium ($\mu_0=1/\sqrt{3}$) and the half space coincide:

$$R(x) \sim \frac{\sqrt{3}}{4}\xi^2 e^{-\xi}, \quad x \to \infty \ . \tag{81}$$

Particles that reach a large depth inside the target must have come there on a more or less straight line, hence at large depths the path length distribution $P(\xi)$—measured in depth units along the incoming direction, $\xi=x/\mu_0=\sqrt{3}x$—and the projected range distribution $R(x)$ should coincide. $P(\xi)$ may be calculated rigorously for hard-sphere scattering.[14,15] It is

$$P(\xi)=\frac{1}{\Gamma\left[1+\frac{1}{2m}\right]}\xi^{1/2m}e^{-\xi}, \quad 0 \le \xi < \infty \ , \tag{82}$$

which coincides for $m=\frac{1}{4}$ apart from a constant factor with (81). This fact enhances our confidence that the qualitative aspects even of the large depth behavior of the particle fluxes are sufficiently well described by a $P_1$ approximation.

In order to assess the accuracy with which the $P_1$ approximation describes the features of half-space transport problems, we solved the linear Boltzmann equation (1) with the Monte Carlo code BEST.[23] All necessary care was taken to ensure that exactly that transport process as described by the Boltzmann equation is simulated. Hard-sphere interaction was employed. The resulting energy spectrum of projectiles emitted from a half space is plotted in Fig. 3 in comparison with the $P_1$ results. As was observed after Eq. (19), in the $P_1$ description of the

half-space problem, no information on the incoming direction $\mu_0$ is available. We therefore ran the Monte Carlo code with an isotropic distribution of incoming directions, thus simulating the boundary condition $\Phi(z=0,E,\mu>0)=\delta(E-E_0)$.

A surprisingly good agreement between the Monte Carlo results and the $P_1$ calculation is observed, particularly at low energies $E$, but also up to near the bombarding energy $E_0$. Further runs were made for several definite values of the incident direction. The asymptotic *slope* is always in agreement with the $P_1$ prediction $s_0$. Not surprisingly, the *number* of particles emitted at low energies is strongly dependent on $\mu_0$; it increases when $\mu_0$ decreases from normal to oblique incidence. Also the *shape* of the high-energy part of the spectrum depends on $\mu_0$: For normal incidence, $j(z=0,E)$ decreases very steeply for $E\rightarrow E_0$, whereas its behavior is much softer for oblique incidence. We thus conclude that the $P_1$ approximation correctly describes the low-energy slope of the emitted particle spectrum for all bombardment directions; it quantitatively describes the whole spectrum, if the projectiles impinge isotropically on the target.

## IX. DISCUSSION

### A. Reliability of the $P_1$ approximation

The method adopted in this paper for the solution of the transport equations for particle slowing down, viz., the $P_1$ approximation, is not meant to allow for a quantitative evaluation of range profiles or reflection and sticking coefficients. Firstly, a number of important physical features are not incorporated into the linear Boltzmann equation (1), such as target (poly)crystallinity and electronic stopping; and secondly, the class of cross sections used here, Eq. (8), approximates the realistic projectile-target interaction only over a limited range of energy for a fixed value of $m$.[1,4] Nevertheless, we think that the $P_1$ approximation is well suited to characterize the basic influence that a free surface exerts on the motion of energetic particles in matter. Since it directly solves the spatial differential equations, it is able to describe certain qualitative aspects of particle penetration phenomena that remain hidden in the method of spatial moments which is often employed. The $P_1$ approximation can to a certain extent incorporate the boundary conditions at the free surface of a half space, and it directly presents the solution for the particle fluxes at the target surface itself.

It may appear strange at first sight that the Marshak boundary condition (18) sets for $E<E_0$ the particle density $\Phi_0$ and current $\Phi_1$ at the surface of a half space proportional to each other, and hence stipulates an identical energy dependence for $\Phi_0(z=0,E)$ and $\Phi_1(z=0,E)$, cf. Eq. (37). The full boundary condition at a free surface, Eq. (17), requires, however, an even stronger interdependence of the Legendre moments $\Phi_l(z=0,E)$ for $E<E_0$: The condition that $\Phi(z=0,E,\mu>0)\equiv 0$ *for all* $\mu>0$ can only be fulfilled if *all* the $\Phi_l(z=0,E)$ *have the same energy dependence.* In a $P_1$ approximation, of course only the coupling between $\Phi_0$ and $\Phi_1$ survives.

Unfortunately, it has not been possible to extend the calculation to higher-order $P_L$ approximations, $L>1$; the difference equations that occur in these cases could not be solved by us. We note, however, that the range distribution at large depths coincides with the path length distribution in a special case of hard-sphere scattering, which is reassuring. The energy distribution at the surface $\Phi_l(z=0,E)$, on the other hand, can be calculated for the case of energy-independent scattering cross sections, i.e., $m=0$, with higher-order $P_L$ ($L\leq 5$) and $DP_L$ approximations ($L\leq 3$); it may be shown that in these cases the $P_1$ approximation already correctly gives the leading term of the asymptotic energy dependence of the particle distributions at the surface of the infinite medium and the half space.[24,25]

Since several weaknesses of the $P_1$ approximation are known in the literature, and particularly in the vicinity of sources and interfaces,[18,15] we solved the Boltzmann equation without any approximation by a numerical solution scheme based on a Monte Carlo approach[23] (Sec. VIII). Since the asymptotic slope of the energy spectrum of reflected particles can be obtained with high precision, and since it is predicted by the present work to deviate characteristically from the well-known infinite-medium value, we took this quantity as the base of our comparison. As discussed in Sec. VIII, the agreement between the numerical results and the prediction of the $P_1$ approximation is fine. On what regards the *absolute values* of the energy spectrum, the $P_1$ approximation obviously describes quite successfully the energy spectrum due to an *isotropic* incident particle distribution, rather than a collimated incident beam, the reason being that the bombarding direction $\mu_0$ is not easily incorporated in a $P_1$ approximation. This certainly constitutes a drawback of the present approach. In order to get some insight into the influence of the bombarding direction $\mu_0$ on the asymptotic slope $s_0$ of the backscattered particle spectrum, we performed a number of calculations with our numerical solution scheme; no variation of $s_0$ with $\mu_0$ could be found.

### B. Energy spectra

Trivially, since particles may leak out of the free surface of a half space without the possibility of returning, which, however, is possible in an infinite medium, the density $\Phi_0$ of particles at the surface of a half space is smaller than the density at the same point in an infinite medium. The current $\Phi_1$ at the half-space surface is outward directed, i.e., negative in our notation. By the same argument as above it is more negative than the corresponding infinite-medium current. It is a salient result of the present paper that, since the above quantities are energy dependent, the same relationships hold for the powers of the asymptotic energy dependence of density and current. Moreover, since at the half-space surface $\Phi(z=0,E,\mu>0)=\sum_{l=0}^{\infty}(2l+1)P_l(\mu)\Phi_l(z=0,E)\equiv 0$ ($E<E_0$), half-space density $\Phi_0$ and current $\Phi_1$ must have the same energy dependence. As we denote the power in the asymptotic energy dependence of the half-space density and current by $s_0$, that of the infinite-medium current by $s_1$, and since for backscattered pro-

jectiles $\Phi_0(z=0,E)\sim E^{1-2m}$ ($E \ll E_0$), we have $s_1 < s_0 < 1-2m$, Eq. (38). Analogously, in the case of sputtered particles, it is $s_1 < s_0 < 2-2m$. Whenever particles do not suffer large angular deflections and hence only few surface crossings in the infinite-medium case, $s_0$ will be close to $1-2m$. This is the case if the projectile reflection coefficient is small, e.g., when the projectile mass is high, or when electronic energy losses are dominant. On the other hand, when the particle motion is diffusive, $s_0$ will be closer to $s_1$, the power describing the infinite-medium current.

We wish to mention that the case $m=0$ has been studied extensively in the literature.[26,24,25] Here the powers $1-2m=1=s_1$ are confluent, and thus only logarithmic deviations occur in the results. While the infinite-medium density behaves as $(E_0/E)(\ln E_0/E)^{-1/2}$ for $E \ll E_0$, the infinite-medium current and both half-space density and current behave as $(E_0/E)(\ln E_0/E)^{-3/2}$, which is in full agreement with the above observations, since in the absence of electronic losses particles never get stuck in the $m=0$ case and the motion therefore may be described as diffusive. A pure power law may be fitted to the $m=0$ particle spectrum with more or less success giving a power less than 1 for the projectiles, and less than 2 for the recoil case.[27,14] We wish to emphasize that such a fit does not do justice to the more delicate behavior described above.

Sputtering from a half space has been studied in an approximate model solution of the transport equation.[28] For special cases the energy spectrum at the target surface could be obtained; it showed deviation from the infinite-medium value in a way consistent with the present results. In particular, the authors showed for these cases that the asymptotic slope of the half-space spectrum, $s_0$ in our notation, lies between $2-4m$ and $2-2m$. Since the equal mass case could not be treated in that reference, a quantitative comparison to our results is not possible.

### C. Range and current distribution

The range distribution is connected to the low-energy limit of the particle flux density divided by $(E_0/E)^{1-2m}$, cf. Eq. (42). Since the half-space density at the target surface follows an asymptotic power law with energy with a power $s_0 < 1-2m$, it follows of necessity that the range distribution vanishes at the surface. It is essential to observe that the vanishing of the range distribution at the target surface and the deviation of the energy spectrum from the $(E_0/E)^{1-2m}$ dependence are intimately connected; each fact can be derived from the other.

The reason the range distribution vanishes near the surface may be visualized in the following way: Particles which come to a stop in the immediate neighborhood of a free surface must have come from inside the target. They must not travel too far, however, for once they trespassed $z=0$ they have no chance to return. Therefore the probability that a particle is stopped at the very surface $z=0$ is vanishingly small, and near to the surface, for $z>0$, it is distinctly lower than in the infinite-medium analog, where also particles coming from $z<0$ may contribute to the range distribution at $z=0$ or $z>0$.

The range distribution decays at the surface as $x^\rho$, $0<\rho<1$; $\rho$ is connected to the power of the asymptotic energy spectrum $s_0$ via Eq. (55): $\rho=(1-2m-s_0)/2m$. According to the discussion above, whenever surface crossings are not essential, i.e., for high projectile mass or dominant electronic stopping, $\rho$ will be close to zero, and the range distribution will steeply decline in the surface region and may for practical purposes be approximated by a jump at the surface. On the other side, when surface crossings are essential, $\rho$ will be larger and the range distribution will decline more gradually towards the surface. Note, however, that $R(x)$ always has an infinite slope at $x=0$.

The current distribution which follows asymptotically a law $(E_0/E)^{s_1}$ for $z \neq 0$, diverges for $z \to 0$ in the half space. The current distribution $\Phi_1$ describes the flux *anisotropy*.[6] While in an infinite medium, the flux anisotropy decays asymptotically for $E \ll E_0$, it remains of the same order of magnitude as the particle density $\Phi_0$ at the surface of a half space. Since $\Phi_1$ is negative at the target surface, more particles are emitted normal to the surface than at oblique angles. Thus the angular spectrum of particles emitted at low energies displays an overcosine behavior.[24,25]

$\Phi_1(z,E)$ changes its sign as a function of $z$: In the vicinity of the surface, particles predominantly move outwards and $\Phi_1<0$, and deep in the target, particles tend to move inwards, so $\Phi_1>0$.[20,25] Thus caution is required if the spatial mean $\Phi_1^0(E)$ is used as an estimate for the magnitude of the flux anisotropy at the target surface. This warning applies even more strongly when the infinite-medium value of $\Phi_1^0$ is used, since it will underestimate the importance of the flux anisotropy at the target surface even more, cf. Eq. (35).

Reference 6 uses an image-type of argument to discuss the surface effect on the deposited-energy distribution, arguing that the particle density at the surface will vanish, while the current will increase by a factor of 2 in comparison with the infinite-medium value. This picture obviously correctly reproduces the basic trends—at least when the reflection coefficient is high—as discussed above and as is also observed in Fig. 2(a).

A number of attempts to estimate the effect of the target surface on slowing-down quantities employ an ingenious connection between the energy spectra (and the slowing-down densities) of the half-space and the infinite-medium solutions. This relationship, which is given in the form of an integral equation, is used to calculate half-space quantities from a knowledge of the infinite-medium solutions; the latter are usually obtained via a spatial moments method. This approach allows the inclusion of realistic scattering cross sections and electronic stopping; it has been applied to the calculation of reflection coefficients,[9] backscattering energy spectra,[10] range distributions,[12] and sputtering quantities.[6] However, no analytical result for energy spectra or range distributions have been made available from these investigations. Qualitatively, the half-space range distributions obtained via this method[12] always lie below their infinite-medium counterparts, in agreement with the conclusions of the present paper. The behavior at the target surface

itself is difficult to investigate via a spatial moments method, and the results presented in Ref. 12 show even a nonzero probability for a projectile to be stopped outside the target.

Very recently Luo and Wang published a numerical calculation of the range distribution of light ions in matter.[29] Their procedure is very different from the present approach, in that they use a continuous slowing-down approximation, separate the collimated and forward scattered part of the incoming beam from the diffusely scattered part, and take care to reach convergence in their numerical scheme, rather than staying at a $P_1$ approximation and looking for analytical results, as we do. The range profiles plotted in that work all display $R(z=0)=0$ at a free surface, in agreement with the present results. Since the approach of Luo and Wang is so different from the present one, and since on the other hand those authors cared to use high-order approximations, we are satisfied that their data corroborate our results.

We refrain from a quantitative comparison of our results with those of other groups studying half-space range distributions[12,29] for the following reasons. First, and most important, the present approach is not meant to yield quantitatively correct range distributions, but rather to display the qualitative changes that a free surface is bound to generate. The main reason for this restriction is the inability of the $P_1$ approximation to handle the bombarding direction $\mu_0$ satisfactorily. Previous methods, in contrast, aim at a quantitative description of range profiles.[12,29] Secondly, the cases where we can obtain an analytical description of the infinite-medium and half-space range distributions, viz., for hard-sphere scattering cross sections in the equal mass case and neglecting electronic stopping, lie far outside the problems studied in Refs. 12 and 29, which are interested in realistic scattering cross sections and light ions, and take into account electronic stopping. We believe that the advantage of the present approach resides rather in its analytical capability than in its quantitative predictivity.

### D. Other influences

Electronic stopping has been entirely neglected in the course of this work, although it definitely influences—particularly at very high bombardment energies—particle motion in matter. The effects we discuss in this paper, namely the low-energy asymptotics of emitted particle spectra and the shape of the range distribution at the very surface, have their origin, however, in *low-energy* particle motion. The value of the electronic stopping power at not too low energies is known to scale as $E^{1/2}$. For power-law scattering, the nuclear stopping scales as $E^{1-2m}$. Thus, for $m>\frac{1}{4}$, it is obviously justified to neglect the effect of electronic stopping. In very-low-energy motion, below 100 eV, say, nuclear stopping may be characterized by a power parameter $m<\frac{1}{4}$, and effects of the electronic stopping on the magnitude of the sputtering yield have been discussed.[30] Experimental data on electronic stopping in this regime are not available, but it seems highly questionable whether electronic stopping follows the $E^{1/2}$ behavior down to such low energies.[31] In view of this uncertainty we refrained from including electronic stopping in our description of low-energy particle motion in matter. Some results on qualitative aspects have been given above.

The effect of the surface barrier on emitted particle spectra is well known and it might easily be included in the present calculations in the standard way.[32,6,3] Because the energy spectra displayed in this work are well described by their asymptotic distribution as soon as $E \lesssim \frac{1}{10}E_0$, measured energy spectra should follow a power law $E^{-s_0}$ for $U \ll E \ll E_0$ ($U$ is the surface binding energy). Apart from surface binding effects, measured sputtered particle spectra follow a power law with energy $\propto E^{-n}$, with $n=2\pm0.1$. It is, therefore, often concluded that the value of $m$ describing low-energy motion in solids must be quite close to zero.[6] We shall discuss these matters further elsewhere.[23]

The validity of the calculated half-space range distributions near to the surface seems to be more questionable, since strong chemical and thermodynamical forces may exist near there which are bound to distort the range distributions described here. We think, however, that when studying the behavior of the range distribution near to a surface, it is useful to start by describing the effects of a surface on the motion of energetic particles in matter, and to include other forces in a second step.

Quite recently, a numerical assessment of the influence of a planar surface barrier on the near-surface range profile of light ions in matter was presented.[33] Since in that case particles which tend to escape the solid with too little perpendicular energy are reflected back into the solid, the surface acts rather as a source of low-energy particles than as a pure drain, such as is the case for a free surface. Consequently, the range distribution in the near-surface regions attain larger values than in the free surface model, and it no longer holds that $R(z=0)=0$.

In the present communication, we obtained an analytical description for the effect of a free surface on energetic particle motion in matter. More quantitative details for a number of realistic interaction cross sections, and taking into account the effects of surface binding, as well as a comparison to existing computer simulation work, will be given elsewhere.[23]

## X. CONCLUSIONS

(1) The transport equations describing the slowing down of an energetic particle in matter, and the generation and slowing down of recoil atoms, are solved in a $P_1$ approximation for the case of a scattering cross section $\sigma(E,T)\propto E^{-2m}$, which obeys a power law in energy.

(2) Results for the range distribution and for the energy spectrum at the target surface are derived, both for an infinite medium and a half space.

(3) The energy spectrum of particles backscattered from a half space behaves asymptotically as $(E_0/E)^{s_0}$ where $E_0$ is the bombardment and $E$ the ejected particle energy ($E \ll E_0$). The power $s_0$ differs from the infinite-medium value; it is between the powers of the infinite-medium particle density, which is $1-2m$, and that of the

infinite-medium current density, which is $1-4m$ for small $m$.

(4) The current has the same asymptotic energy dependence as the particle density; thus the flux remains anisotropic at the very target surface even at very low energies $E$. This is in contrast to the behavior in an infinite medium, where the angular distribution becomes isotropic.

(5) The range distribution declines to zero at the half-space surface as $x^{\rho}$, where $x$ is the depth inside the target, and $0<\rho<1$. $\rho$ is closely connected to the asymptotic slope $s_0$ of the energy spectrum at the target surface.

(6) If the reflection coefficient of the projectile is small, e.g., for a high projectile mass or for dominant electronic stopping, $s_0$ is close to $1-2m$, and $\rho \simeq 0$. For a small projectile mass, and negligible electronic stopping, the deviations from the infinite-medium behavior are more pronounced.

(7) The analogous results hold for the energy spectrum of sputtered particles and the deposited-energy distribution.

(8) As an illustration, analytical results for half-space and infinite-medium range distributions and energy spectra for the case of equal mass hard-sphere scattering with the scattering cross section depending on energy like $E^{-1/2}$ ($m=\frac{1}{4}$) are derived. These are confirmed by a numerical solution of the linear Boltzmann equation via a Monte Carlo simulation.

## ACKNOWLEDGMENTS

Thanks are due to Bruce Winterbon for drawing our attention to Ref. 15. One of the authors (M.V.) acknowledges financial assistance by the Deutsche Forschungsgemeinschaft.

[1] J. Lindhard, V. Nielsen, and M. Scharff, K. Dan. Vidensk. Selsk., Mat. Fys. Medd. **36**, No. 10 (1968); J. Lindhard, M. Scharff, and H. E. Schiøtt, *ibid.* **33**, No. 14 (1963); J. Lindhard, V. Nielsen, M. Scharff, and P. V. Thomsen, *ibid.* **33**, No. 10 (1963).

[2] D. K. Brice, *Ion Implantation Range and Energy Deposition Distributions* (Plenum, New York, 1975), Vol. 1; K. B. Winterbon, *Ion Implantation Range and Energy Deposition Distributions* (Plenum, New York, 1975), Vol. 2.

[3] E. S. Mashkova and V. A. Molchanov, *Medium-Energy Ion Reflection from Solids* (North-Holland, Amsterdam, 1985).

[4] P. Sigmund, Phys. Scr. **28**, 257 (1983).

[5] K. B. Winterbon, P. Sigmund, and J. B. Sanders, K. Dan. Vidensk. Selsk., Mat. Fys. Medd. **37**, No. 14 (1970).

[6] P. Sigmund, in *Sputtering by Particle Bombardment I,* edited by R. Behrisch (Springer, Berlin, 1981), p. 9.

[7] K. B. Winterbon and J. B. Sanders, Radiat. Eff. **39**, 39 (1978).

[8] D. K. Brice, Nucl. Instrum. Methods B **17**, 289 (1986).

[9] J. Bøttiger, J. A. Davies, P. Sigmund, and K. B. Winterbon, Radiat. Eff. **11**, 69 (1971).

[10] U. Littmark and A. Gras-Marti, Appl. Phys. **16**, 247 (1978).

[11] M. Imada, J. Phys. Soc. Jpn. **45**, 1957 (1978).

[12] S. Fedder and U. Littmark, J. Appl. Phys. **52**, 4259 (1981).

[13] U. Littmark and G. Maderlechner, in *Physics of Ionized Gases, Book of Contributed Papers,* edited by B. Navinsek (J. Stefan Institute, Dubrovnik, 1976), p. 139.

[14] M. M. R. Williams, Prog. Nucl. Energy **3**, 1 (1979).

[15] K. B. Winterbon, Radiat. Eff. **39**, 31 (1978).

[16] G. Leibfried, *Bestrahlungseffekte in Festkörpern* (Teubner, Stuttgart, 1965); D. K. Holmes and G. Leibfried, J. Appl. Phys. **31**, 1046 (1960).

[17] P. Sigmund and J. B. Sanders, in *Proceedings of the International Conference on Applications of Ion Beams to Semiconductor Technology,* edited by P. Glotin (Editions Ophrys, Paris, 1967), p. 215.

[18] B. Davison, *Neutron Transport Theory* (Oxford University Press, London, 1957); K. M. Case and P. F. Zweifel, *Linear Transport Theory* (Addison-Wesley, Reading, 1967).

[19] I. Waller, Ark. Fys. **37**, 569 (1968).

[20] U. Littmark and P. Sigmund, J. Phys. D **8**, 241 (1975); H. E. Roosendaal, U. Littmark, and J. B. Sanders, Phys. Rev. B **26**, 5261 (1982).

[21] M. M. R. Williams, *The Slowing Down and Thermalization of Neutrons* (North-Holland, Amsterdam, 1966).

[22] *Handbook of Mathematical Functions,* edited by M. Abramowitz and I. A. Stegun (Natl. Bur. Stand., Washington D.C., 1965).

[23] M. Vicanek and H. M. Urbassek, Nucl. Instrum. Methods B (to be published).

[24] K. T. Waldeer and H. M. Urbassek, Nucl. Instrum. Methods B **18**, 518 (1987).

[25] K. T. Waldeer and H. M. Urbassek, Appl. Phys. A **45**, 207 (1988).

[26] M. Urbassek, Nucl. Instrum. Methods B **4**, 356 (1984); **6**, 585 (1985).

[27] M. M. R. Williams, Philos. Mag. A **43**, 1221 (1981).

[28] I. Lux and I. Pászit, Radiat. Eff. **59**, 27 (1981).

[29] Z. Luo and S. Wang, Phys. Rev. B **36**, 1885 (1987).

[30] M. M. Jakas and D. E. Harrison, Jr., Phys. Rev. B **32**, 2752 (1985).

[31] P. Sigmund, Nucl. Instrum. Methods B **27**, 1 (1987).

[32] M. W. Thompson, Philos. Mag. **18**, 377 (1968).

[33] Z. Luo (unpublished).